

# Near Infrared Molecular Imaging of Breast Cancer Cell Lines Using a Novel ER Targeted Fluorescent Dye

Vinay Jha Pillai (✉ [vinay.pillai@christuniversity.in](mailto:vinay.pillai@christuniversity.in))

Christ University Faculty of Engineering <https://orcid.org/0000-0002-0693-2234>

Iven Jose

Christ University Faculty of Engineering

---

## Research Article

**Keywords:** Breast Cancer, Estrogen Receptor, fluorescent dye, MCF-7, MDA MB 231, Near-infrared

**Posted Date:** February 18th, 2022

**DOI:** <https://doi.org/10.21203/rs.3.rs-1337574/v1>

**License:**  This work is licensed under a Creative Commons Attribution 4.0 International License.

[Read Full License](#)

---

# Abstract

Hormone-targeted contrast agents bind with functional groups associated with the physiology of breast cancer leading to improved prognosis. We have synthesized a novel estrogen receptor (ER) targeted near-infrared fluorescent dye referred to as Novel Dye Conjugate (nDC). It is a conjugate of 17 $\beta$ -estradiol with a derivative of indocyanine green dye, bis-1,1-(4-sulfobutyl) indotricarbocyanine-5-carboxylic acid, sodium salt. Structural and photophysical characterizations of nDC followed with breast cancer cell lines (MCF-7 and MDA MB 231) stained with novel dye were carried out. The target, MCF-7 cells (ER-positive) showed specific high-affinity binding sites of novel dye onto the nucleus and membrane of ER-positive cells, in contrast, the control, MDA MB 231 (ER-negative) showed only plasma membrane staining. Similar results were obtained when ER expressing cancerous tissues (viz. Non-Invasive Ductal Carcinoma, Non-Invasive Lobular Carcinoma, Non-Invasive Adenocarcinoma, and Non-Invasive Medullary Carcinoma) were stained with novel dye. Approximately 70% of breast cancer cases are ER-positive, therefore nDC being ER binding properties can unambiguously improve the specificity and sensitivity of breast cancer imaging.

## 1. Introduction

Molecular imaging tools have opened up a wide possibility of early cancer detection by letting scientist/physician visualize the human body at the cellular and molecular level [1-5]. Molecular imaging with the help of contrast agents/biomarkers not only provides clinicians with location of cancerous cells but also the information of other biological processes that influences the malignancy [6-10]. The exploration of contrast agents with emission wavelength in NIR region started to find a profound application in biomedical molecular imaging application [11-16]. One such popular and extensively used clinically approved NIR dye is Indocyanine green (ICG) [17-21]. Ntziachristos showed that ICG has profound application as a contrast agent in optical imaging for breast cancer detection [22]. But it has poor tumor localizing properties [23], insufficient aqueous solution stability [24] accompanied by low fluorescence efficiency [25]. Thus, suggesting a need for synthesizing probe with significantly increased hydrophilicity compared to ICG. One such prominent study incorporating the above requirements were carried out by Licha et al [26]. They synthesized compounds which were modified derivatives of ICG had less protein plasma binding with increased hydrophilicity and enhanced fluorescence quantum yield. Also, these compounds had a better pharmacokinetic property compared with ICG. One of the compounds synthesized was Bis-1,1 9-(4-sulfobutyl) indotricarbocyanine-5-carboxylic acid, sodium salt, which was extensively used in our research. Although, glucosamine substituted dye which had improved hydrophilicity, but it lacked in the capability of differentiating the malignant cell from benign along with poor cell endocytosis. Therefore, there was a need for contrast agent capable of nuclear level staining which was possible by tagging cyanine dye with a functional group having affinity to bind with hormones over-expressed in the nuclei of the cancerous cells. This lead for need to identify a potent functional group which could be tagged with the cyanine dye to improve specificity and sensitivity of breast cancer diagnostic modality. The tumors over-express specific receptors which differentiate tumor from normal cell. Estrogen Receptor (ER) are a group of proteins found inside the nucleus of the cell which is activated

by estradiol. Also, studies showed that 70% of breast cancerous cell express ER [27 and 28]. Hence, it is clear that targeting ER can help in the prognosis of breast cancer. Boothby et al [29] had established the binding ability of bioidentical estrogen viz. 17 $\beta$  Estradiol with ER. Thus, the inception of estradiol conjugated cyanine dye was conceived in [30 and 31].

Following sections details the synthesis of novel target specific fluorescent dye, validation of its structure and photophysical properties. Thereafter, sensitivity and specificity of novel dye is proven through cancer cell lines and tissue studies.

## 2. Synthesis Of Novel Dye Conjugate

Synthesis on Novel Dye Conjugate (nDC). In the present study, the novel dye conjugate was synthesized by ester formation between 17- $\beta$  estradiol and a hydrophilic derivative of indocyanine green (ICG) viz. bis-1, 1-(4-sulfonylbutyl) indotricarbocyanine-5- carboxylic acid, sodium salt. Steps involved in the synthesis of the conjugate of estradiol with a cyanine derivative are as follows. The synthesis involved nine step procedure which starts with stirring of 4-Phenyl-1,2,3,6-tetrahydro-pyridine (C11H13N) with Hydroperoxythioxane in the presence of 1,2-Dichlorobenzene at 1800C for 14 hours. Key steps involved in the synthesis processes are discussed here and are also displayed in Fig. 1. A solution of 17 $\beta$ -Estradiol (357mg, 1.311mmol), EDC.HCl (244 mg, 1.573 mmol) and dimethylaminopyridine were added to bis 1,1-(4-sulfonylbutyl) indotricarbocyanine-5-carboxylic acid sodium (400 mg, 0.524 mmol) solution in presence of dry dimethylformamide (4.0 mL) (Fig. 1 (a) and (b)). The above reaction mixture was stirred at about 24 hours at 25°C. Upon completion of the reaction, the reaction mass was poured into hot ether. The resultant solid filtered to get the crude compound. The crude obtained was further purified by reverse phase column chromatography to get pure compound (126mg, 10%) as pale green solid (Fig. 1 (c)). The solution of this compound (0.043 mmol, 55 mg) was added with trimethylamine (0.098 mmol, 9.93 mg) and D-glucosamine hydrochloride (10.26 mg, 0.0475 mmol) in the presence of dry dimethylformamide (700  $\mu$ L) at about 0°C. The mixture was stirred for 2hours at about 25°C. The resulting reaction mass was poured to methyl tert-butyl ether (MTBE). MTBE solvent is decanted, and the residue is kept for lyophilization for three days to afford 53 mg of the final compound as green solid as shown in Fig. 1 (e). The present study claims novelty in the esterification procedure as solely administered by the lab (research group at Photonics Lab, CHRIST (Deemed to be University)), wherein the hydroxyl group of ICG derivative was replaced by 17- $\beta$  estradiol forming symmetric structure, which is not reported elsewhere.

The final compound, hereafter referred as Novel Dye Conjugate (nDC), has a molecular mass of 1428.78714 g/mol with large structure at the center corresponding to ICG derivative. Also, the NA<sup>+</sup> ion in the ester was replaced by D-Glucosamine hydrochloride in order to improve hydrophilicity and reduce cytotoxicity. Novel molecule is completely soluble in DMSO and PBS solutions and has exhibited its fluorescence properties to be in near-infra red region. US patent has been granted for the synthesis steps [32].

## 3. Validation Of Ndc Formation (Lcms And H1nmr)

Liquid Chromatography–Mass Spectrometry (LC-MS) technique was used to analyze the final compound synthesized (conjugate). Fig. 2 (a) shows LC results for the final compound synthesized. A 53 mg of the final target molecule (nDC) was synthesized with 98.6% LC purity. Here, purity percentage was calculated based on the relative area under the graph at the time 3.945 (AU) on the X-axis. Other molecules were retrieved with 1.175% and 0.254% purity with relatively low concentration at time 3.2 (AU) and 3.42 (AU), respectively. Once separated in the LC process, the components were converted to an ionized state.

In the next step, i.e. Mass Spectrometry (MS), involves identification of components based on the mass to charge ratio ( $m/z$ ) as a characterizing factor. Fig. 2 (b) shows the mass to charge ratio plotted against the peak intensity. As indicated in the figure, the parent ion mass corresponding to  $m/z$ : 1250 in the positive mode with purity of 98.6% is obtained using LC/MSD Trap XCT Ultra equipment. Impurities of 1.4% around  $m/z$ :1308.9 is also seen in Fig. 2 (b). Hydrogen-1 Nuclear Magnetic Resonance (1H-NMR) technique was used to confirm the molecular identity and structure of the final molecule for further validation. 1H-NMR spectrum for nDC is shown in Fig. 3 which was recorded at 400MHz NMR spectrometer. Results clearly indicates the presence of key groups viz. D-Glucosamine,  $17\beta$  Estradiol, Sultone group etc.

## 4. Photophysical Properties

Photophysical properties of the novel dye were studied by dissolving it in dimethyl sulfoxide (DMSO) and phosphate buffered saline (PBS). DMSO and PBS are generally used solvent for biological studies since its properties match with human body fluids. Peak absorption and emission wavelength were recorded using VARIOSKAN LUX Multimode Microplate Reader of Thermo Scientific make. Absorption and emission peak of novel dye was observed to be in NIR region with a 30 nm Stokes's shift (Table 1). Excitation and emission wavelengths were observed to be at 757nm and 787nm in DMSO, respectively. The results also support the independence of dye concentration on peak absorption wavelength, which confirms the stability of the dye in the solvent.

## 5. In-vitro Studies Using Breast Cancer Cell Lines

Hereafter, the sections will showcase the study of breast cancer cell-lines with our novel dye administered. Since the present study involves establishing the binding properties of nDC with Estrogen receptors we chose MCF-7 (target): Estrogen receptors (ER) positive and MDA MB 231 (control): Triple Negative (ER, PR and HER negative) cell lines for our studies. Both are human breast tissue cell lines from mammary gland with adenocarcinoma. The main difference between the two cell lines is that MCF-7 (target) expressed estrogen receptor, whereas MDA MB 231 (control) did not express the same. The motive of choosing the above cell lines was to prove that novel dye had a specific binding affinity with ER-positive cell lines (MCF-7). And also, to show that there was no specific binding with ER-negative cell lines (MDA MB 231).

### 5.1 Cytotoxicity Studies

The cytotoxicity studies aimed to determine the viability of the cells post nDC administration. As discussed earlier, breast cancer cell lines chosen were MCF-7 and MDA-MB-231. A 30 mM stocks of nDC were made in DMSO. On day 1, a 96-well plate for cell seeding density of 10,000 cells/well was prepared with 100 µL of complete medium (Dulbecco's Modified Eagle Medium with 10% fetal bovine serum). An incubation condition in 5% CO<sub>2</sub> was set at 37°C for 24 hours. On day 2, the nDC ester was weighed, and a 30 mM of working stock was made in DMSO with 1% FBS. Test sample concentrations of 10, 20, 30, 40, 50, 60, 70, 80, 90, 100 µM of nDC were prepared and the cells were treated with the same. Fig. 4 shows the viability of cell for the various concentrations over 24 hours. Based on the above figure, it is evident that dose-dependent cell cytotoxicity was not observed for our novel dye in MCF-7 and MDA-MB-231 cells in the tested range of 10-100 µM up to 24-48 hours of treatment. On average, 90% of cells were viable after 24-48 hours of dye treatment. Hence, the novel dye proved negative in toxicity which enabled us to proceed with further studies.

## 5.2 Specific Binding Studies

In this section, we discuss some of our significant findings for endocytosis of the novel dye conjugate in the cell lines and its specific binding. DMEM/F12 medium was used to culture MDA MB 231 and MCF 7 with 10% fetal bovine serum in absence of phenol red. Each of 96-well culture plate were added with 50 µL cell suspension for a final 1x10<sup>3</sup> cells/well concentration which was incubated in carbon dioxide chamber at 37° C for 24 hours. Each well was added with 24.5mg/2ml of DMSO initial concentration and nDC, which were further incubated for 2 hours. Different concentration of DMSO (1:10, 1:50, 1:100, 1:500 and 1: 1000) were used to treat cell thereafter, and were incubated at about 25°C for an hour. Thereafter, cells were given three washes of phosphate buffered saline and were mounted with DPX (Distrene Plasticryser Xylene). These were then imaged using the Olympus Confocal microscope. We carried out in total of three tests with cell lines:

Test 1: Confocal imaging of the cell lines post nDC administration.

Test 2: Confocal imaging of the cell lines administered with nDC post Diethylstilbestrol (DES) and Tamoxifen Treatment.

Test 3: Confocal imaging of MCF-7 stained with ICG

- Test 1: Cell Lines Administered with nDC

Both the cell lines were stained with novel dye conjugate. Fig. 5(a) shows the confocal images of MCF-7 cell lines stained with nDC. Fig. 5(b) is a DIC image of 5(a). It can be observed that the fluorescent intensity at the nucleus is higher in comparison to the background. Localization of conjugated dye in the nucleus of MCF-7 (ER-positive) cell lines is evident in Fig. 5(a). The cell proliferation is controlled by estrogen. The functional group associated with the dye is instrumental in percolating the dye into the nucleus of MCF-7 cell lines and hence providing a unique distinction between the cells and background. Fig. 5(c) shows the confocal images of MDA MB 231 cell lines stained with nDC. These cell lines lack the

estrogen activity in the nucleus therefore, it can be observed from the figure evidently that the fluorescent intensity at the nucleus is lower in comparison to the background. The fluorescence signal largely co-localized in the cytoplasm of the cells. Hence, the control, MDA-MB-231 showed staining only at the levels of the plasma membrane. Clearly, nDC endocytosis failed due to absence of estrogen receptors. From the above test, it is clear that nDC has a special binding ability with cancerous cell exhibiting estrogen receptors. Further to prove our claim, we carried out a test wherein the cell lines were treated with antagonist drugs as explained in the next section.

- Test 2: DES and Tamoxifen Treatment

Diethylstilbestrol (DES) and Tamoxifen are commonly used antagonist drugs which blocks the estrogen receptors from binding with estrogens. MCF 7 cells were treated with various concentrations of DES and Tamoxifen separately for five days. Fig. 5(e) is confocal image of MCF-7 cell lines treated with DES then stained with nDC. Fig. 5(d) is confocal images of MCF-7 cell lines treated with Tamoxifen then stained with nDC. From both the images, it is evident that fluorescence signal is high at the cytoplasm and low in the nucleus. It clearly demonstrates that the nDC is blocked from entering the nucleus due to blocking of ER activity by DES and Tamoxifen treatment respectively. Hence, from test 1 and 2, it can be concluded that the entry of nDC was facilitated due to the presence of active estrogen receptors making our novel dye a target specific.

- Test 3: ICG Staining of MCF-7

Indocyanine Green (ICG) is the commercially available nonspecific fluorescent dye. Fig. 5(f) shows cytoplasm level staining of MCF-7 cell lines by ICG as expected. The fluorescence signal is as low as nil at the center of the nucleus with high intensity in the cytoplasm. It shows an apparent distinction on non-specific binding when compared to specific binding of nDC. Thus, it proves that the nDC is superior in term of specificity of target enhancement.

## 6. Tissue Studies

We obtained following cancer tissues for our studies: Non-Invasive Ductal Carcinoma, Non-Invasive Lobular Carcinoma, Non-Invasive Adenocarcinoma, Non-Invasive Medullary Carcinoma, all of which expressed estrogen receptors. Paraffin sections of said human cancer tissues were fixed in cold buffered formalin through avidin-biotin-peroxidase complex method. These sections were used to demonstrate ER and compared with respective tumor tissue ER content. The tumor pieces were fixed in pH 7.4/10% formalin and 0.1 M sodium phosphate (buffered formalin) for 24 hours at 40°C. Then, the tissues were rinsed in 0.1 M sodium phosphate (pH 7.4) overnight at 40°C, thereafter dehydrated using graded ethanol followed by embedding tissues into paraffin. A 4 $\mu$ m thin sections of paraffin were cut followed by deparaffinization and thorough rinsing with xylene and absolute ethanol respectively. The endogenous peroxidase activity was decreased by soaking the thin sections in absolute methanol with 0.3% H<sub>2</sub>O<sub>2</sub> for 30 minutes at 25°C room temperature. The nonspecific staining was reduced by washing the sections

with 50 mM Tris-HCl, pH 7.6/137 mM NaCl (Tris/NaCl) thrice and then they were incubated in serum (10% in Tris/NaCl) for 30 minutes at 25°C. Excess serum was removed by blotting at 37°C for 30 minutes. Subsequently another washing with 50 mM Tris-HCl, pH 7.6/137 mM NaCl (Tris/NaCl) was carried out followed by reaction with 3,3'-diaminobenzidine tetrahydrochloride (DAB) solution (0.05 M ammonium acetate/citric acid, pH 5.5-6.0) containing 0.0075% H<sub>2</sub>O<sub>2</sub> and 0.2 mg of DAB per ml) for color development in the dark for six minutes.

About 5–72% of ER-Positive cells were observed in paraffin sections of ER positive tissues. The nuclear staining of nDC specific to ER is positive in most of the tumors in the paraffin sections. In Figure 6, ER binding of nDC with non-invasive ductal carcinoma and non-invasive lobular carcinoma is shown. Fig. 6(a and c) shows respective tissue (control) which is not treated with nDC and Fig. 6(b and d) shows respective specific nuclear biding of nDC upon staining. Fig. 6 shows nDC binding with ER in the Non-Invasive Adenocarcinoma (Fig. 6 (a) & (b)) and Medullary Carcinoma (Fig. 6 (c) & (d)). Specific nuclear binding of nDC is seen in respective carcinoma. In all the four cancer tissues, nuclear level staining was observed for ER positive cell diffusely, hence proving the ability of nDC to bind with estrogen receptor positive cells. but the intensity of the nuclear staining was not homogeneous within a section. The heterogenous distribution of nuclear level biding of nDC and intensity did not correspond to differences in tumor histology. Although the frozen sections show no cytoplasmic staining, a few paraffin sections do. Furthermore, the negative controls of paraffin sections show no nuclear staining. Because it exists in the negative control sections, a faint staining is noticed occasionally in connective tissue, necrotic tissue, leukocytes, and erythrocytes is also deemed nonspecific. Hence from above tissue study results, it can be observed that the target specific binding of our novel dye is established further proving it to be a unique and potential probe for breast cancer detection.

## Conclusion

Novel ER targeted fluorescent dye was synthesized successfully through tagging of 17β-Estradiol to a hydrophilic Bis-1,1 9-(4-sulfonylbutyl) indotricarbocyanine-5-carboxylic acid, sodium salt. The structure of the final compound (nDC) was confirmed through LC-MS and 1H-NMR techniques. Photophysical properties confirmed the emission and excitation wavelength of nDC in NIR region and proven to be stable in the solvents like DMSO and PBS. MCF-7 and MDA MB 231 cell lines were used as target and control respectively to study specific binding properties of the novel dye. Cytotoxicity studies proved that the 90% cells were viable ever after 24-48 hours of administration of nDC into the MCF-7 and MDA MB 231 cell lines. Thus, proving it to be safe for the biological administration. Confocal imaging of cell lines stained with nDC showed the specific nuclear binding of novel dye with ER cancer cells. As shown earlier, nuclear level staining of nDC proved the endocytosis of novel dye into the nucleus of MCF-7. Hence, making the dye ER target specific which improves the sensitivity of dye in cancer cell detection. In comparison to ICG, which stained only to the level of cytoplasm, nDC proved to be a powerful contrast agent with a high scope of early detection of cancer cells. Further studies upon treatment of cell lines with DES and Tamoxifen showed poor endocytosis of nDC into nucleus due to blocked ER activities.

Therefore, again proving the specificity of nDC. Tissue studies also showed the specific binding of nDC within the nucleus of ER-positive cells. Thus, with the above conclusion, it is evident that specific binding properties of nDC with ER-positive cells can prove to be significant advantages for the detection of cancer cells. Its high sensitivity and specificity can complement diagnostic tools in imaging the cancer cells with great accuracy with the possibility of early diagnosis of cancer.

## Declarations

### Acknowledgment

We acknowledge the support offered by Dr. S V Chiplunkar, Former Director of ACTREC, Mumbai and Mrs. Meena, Staff at ACTREC, Mumbai to carry out cell lines and tissue studies.

### Funding

This work was supported in parts by the major research project grant MRP DSC 1109 (INR 21 lakhs ) and MRPENG 1812 (INR 6 Lakhs), Centre for Research (Projects), CHRIST (Deemed to be University), Bangalore, 560029

### Competing Interests

The authors have no relevant financial or non-financial interests to disclose.

### Conflicts of Interest/Competing Interests

The authors have no conflicts of interest to declare that are relevant to the content of this article.

### Author Contributions

All authors contributed to the study conception and design equally.

**Data Availability:** Not applicable.

**Code Availability:** Not applicable.

**Ethics Approval:** Not Applicable.

**Consent to Participate:** Not Applicable.

**Consent for Publication:** Not Applicable.

## References

1. Covington MF et al (2022) Advances and Future Directions in Molecular Breast Imaging. Journal of Nuclear Medicine. 63(1): 17-21. <https://doi.org/10.2967/jnumed.121.261988>

2. Han Z et al (2021) Molecular Imaging, How Close to Clinical Precision Medicine in Lung, Brain, Prostate and Breast Cancers. *Molecular Imaging and Biology*. 1-15. <https://doi.org/10.1007/s11307-021-01631-y>
3. Munck S et al (2021) Maximizing content across scales: Moving multimodal microscopy and mesoscopy toward molecular imaging. *Current Opinion in Chemical Biology*. 63: 188-199. <https://doi.org/10.1016/j.cbpa.2021.05.003>
4. Zhou W et al (2021) The application of molecular imaging to advance translational research in chronic inflammation. *Journal of Nuclear Cardiology*. 28(5): 2033-2045. <https://doi.org/10.1007/s12350-020-02439-z>
5. Zheng G, Dai Z (2020) Molecular imaging. *Bioconjugate Chemistry*. 31(2): 157-158. <https://doi.org/10.1021/acs.bioconjchem.0c00044>
6. Mieog, JS D et al (2022) Fundamentals and developments in fluorescence-guided cancer surgery. *Nature Reviews Clinical Oncology*. 19(1): 9-22. <https://doi.org/10.1038/s41571-021-00548-3>
7. Mendive-Tapia L, Wang J, Vendrell M. (2021). Fluorescent cyclic peptides for cell imaging. *Peptide Science*. 113(1): e24181. <https://doi.org/10.1002/pep2.24181>
8. Tolmachev V, Orlova A, Sørensen J (2021) The emerging role of radionuclide molecular imaging of HER2 expression in breast cancer. *Seminars in Cancer Biology* 72: 185-197 <https://doi.org/10.1016/j.semcancer.2020.10.005>
9. Shuvaev S, Akam E, Caravan P (2021) Molecular MR contrast agents. *Investigative Radiology*, 56(1), 20-34. <https://doi.org/10.1097/rli.0000000000000731>
10. Upputuri, PK, Pramanik M (2020) Recent advances in photoacoustic contrast agents for in vivo imaging. *Wiley Interdisciplinary Reviews: Nanomedicine and Nanobiotechnology*. 12(4): e1618. <https://doi.org/10.1002/wnan.1618>
11. F. F. Jobsis (1977) Noninvasive infrared monitoring of cerebral and myocardial sufficiency and circulatory parameters. *Science* 198:1264-1267. <https://doi.org/10.1126/science.929199>
12. Hu Z, Chen WH, Tian J, Cheng Z (2020) NIRF nanoprobes for cancer molecular imaging: approaching clinic. *Trends in Molecular medicine*. 26(5): 469-482. <https://doi.org/10.1016/j.molmed.2020.02.003>
13. Huang J, & Pu K (2021) Near-infrared fluorescent molecular probes for imaging and diagnosis of nephro-urological diseases. *Chemical Science*. 12(10): 3379-3392. <https://doi.org/10.1039/D0SC02925D>
14. Khaishah, H., & Jaffer, F. A. (2020). Intravascular molecular imaging: Near-infrared fluorescence as a new frontier. *Frontiers in Cardiovascular Medicine*, 7, 285. <https://doi.org/10.3389/fcvm.2020.587100>
15. Kennedy GT et al (2021). Use of near-infrared molecular imaging for localizing visually occult parathyroid glands in ectopic locations. *JAMA Otolaryngology–Head & Neck Surgery*, 147(7), 669-671. <https://doi.org/10.1001/jamaoto.2021.0615>
16. Wan H, Du H, Wang F, Dai H. (2019). Molecular Imaging in the Second Near-Infrared Window. *Advanced Functional Materials*, 29(25), 1900566. <https://doi.org/10.1002/adfm.201900566>

17. Fujimoto, S. et al (2021). Indocyanine green-labeled dasatinib as a new fluorescent probe for molecular imaging of gastrointestinal stromal tumors. *Journal of Gastroenterology and Hepatology*, 36(5): 1253-1262. <https://doi.org/10.1111/jgh.15281>
18. Dumitru D, Ghanakumar S, Provenzano E, Benson, JR (2022). A Prospective Study Evaluating the Accuracy of Indocyanine Green (ICG) Fluorescence Compared with Radioisotope for Sentinel Lymph Node (SLN) Detection in Early Breast Cancer. *Annals of Surgical Oncology* 1-7. <https://doi.org/10.1245/s10434-021-11255-9>
19. Abe H et al (2011) Indocyanine green fluorescence imaging system for sentinel lymph node biopsies in early breast cancer patients. *Surgery Today*. 41(2): 197-202. <https://doi.org/10.1007/s00595-009-4254-8>
20. Lin J et al (2020) Indocyanine green fluorescence method for sentinel lymph node biopsy in breast cancer. *Asian Journal of Surgery*. 43(12): 1149-1153. <https://doi.org/10.1016/j.asjsur.2020.02.003>
21. Onda, N, Kimura M, Yoshida T, Shibutani M. (2016). Preferential tumor cellular uptake and retention of indocyanine green for in vivo tumor imaging. *International journal of cancer*, 139(3), 673-682. <https://doi.org/10.1002/ijc.30102>
22. Ntziachristos V, Yodh AG, Mitchell S, Chance B (2000) Concurrent MRI and diffuse optical tomography of breast after indocyanine green enhancement. *Proceedings of the National Academy of Sciences*. 97(6):2767-2772. <https://doi.org/10.1073/pnas.040570597>
23. Meijer DKF, Weert B, Vermeer GA (1988) Pharmacokinetics of biliary excretion in man. VI. Indocyanine green. *European Journal of Clinical Pharmacology*. 35(3): 295-303. <https://doi.org/10.1007/BF00558268>
24. Landsman ML, Kwant G, Mook GA, Zijlstra WG (1976). Light-absorbing properties, stability, and spectral stabilization of indocyanine green. *Journal of Applied Physiology*. 40(4): 575-583. <https://doi.org/10.1152/jappl.1976.40.4.575>
25. Soper SA, Mattingly QL (1994) Steady-state and picosecond laser fluorescence studies of nonradiative pathways in tricarbocyanine dyes: implications to the design of near-IR fluorochromes with high fluorescence efficiencies. *Journal of the American Chemical Society*. 116(9); 3744-3752. <https://doi.org/10.1021/ja00088a010>
26. Licha K et al (2000). Hydrophilic Cyanine Dyes as Contrast Agents for Near-infrared Tumor Imaging: Synthesis, Photophysical Properties and Spectroscopic In vivo Characterization. *Photochemistry and Photobiology*. 72(3): 392-398. [https://doi.org/10.1562/0031-8655\(2000\)072<0392:hcdaca>2.0.co;2](https://doi.org/10.1562/0031-8655(2000)072<0392:hcdaca>2.0.co;2)
27. Nadji M, Gomez-Fernandez C, Ganjei-Azar P, Morales AR(2005). Immunohistochemistry of estrogen and progesterone receptors reconsidered: experience with 5,993 breast cancers. *American Journal of Clinical Pathology*. 123(1): 21-27. <https://doi.org/10.1309/4wv79n2ghj3x1841>
28. Bai, J. W., Wei, M., Li, J. W., & Zhang, G. J. (2020). Notch signaling pathway and endocrine resistance in breast cancer. *Frontiers in Pharmacology*, 11, 924. <https://doi.org/10.3389/fphar.2020.00924>

29. Boothby LA, Doering, PL, Kipersztok S (2004). Bioidentical hormone therapy: a review. Menopause, 11(3): 356-367. <https://doi.org/10.1097/01.gme.0000094356.92081.ef>
30. Jose I, Deodhar KD, Desai UB, Bhattacharjee S (2011). Early detection of breast cancer: synthesis and characterization of novel target specific NIR-fluorescent estrogen conjugate for molecular optical imaging. Journal of Fluorescence, 21(3): 1171-1177. <https://doi.org/10.1007/s10895-010-0795-x>
31. Schouw, H. M. et al (2021). Targeted optical fluorescence imaging: a meta-narrative review and future perspectives. European Journal of Nuclear Medicine and Molecular Imaging, 48(13), 4272-4292. <https://doi.org/10.1007/s00259-021-05504-y>
32. Jose I, Chiplunkar SV, Pillai V J, Verma R (2018). Conjugate of estradiol and applications thereof. U.S. Patent No. 10,054,602. Washington, DC: U.S. Patent and Trademark Office.

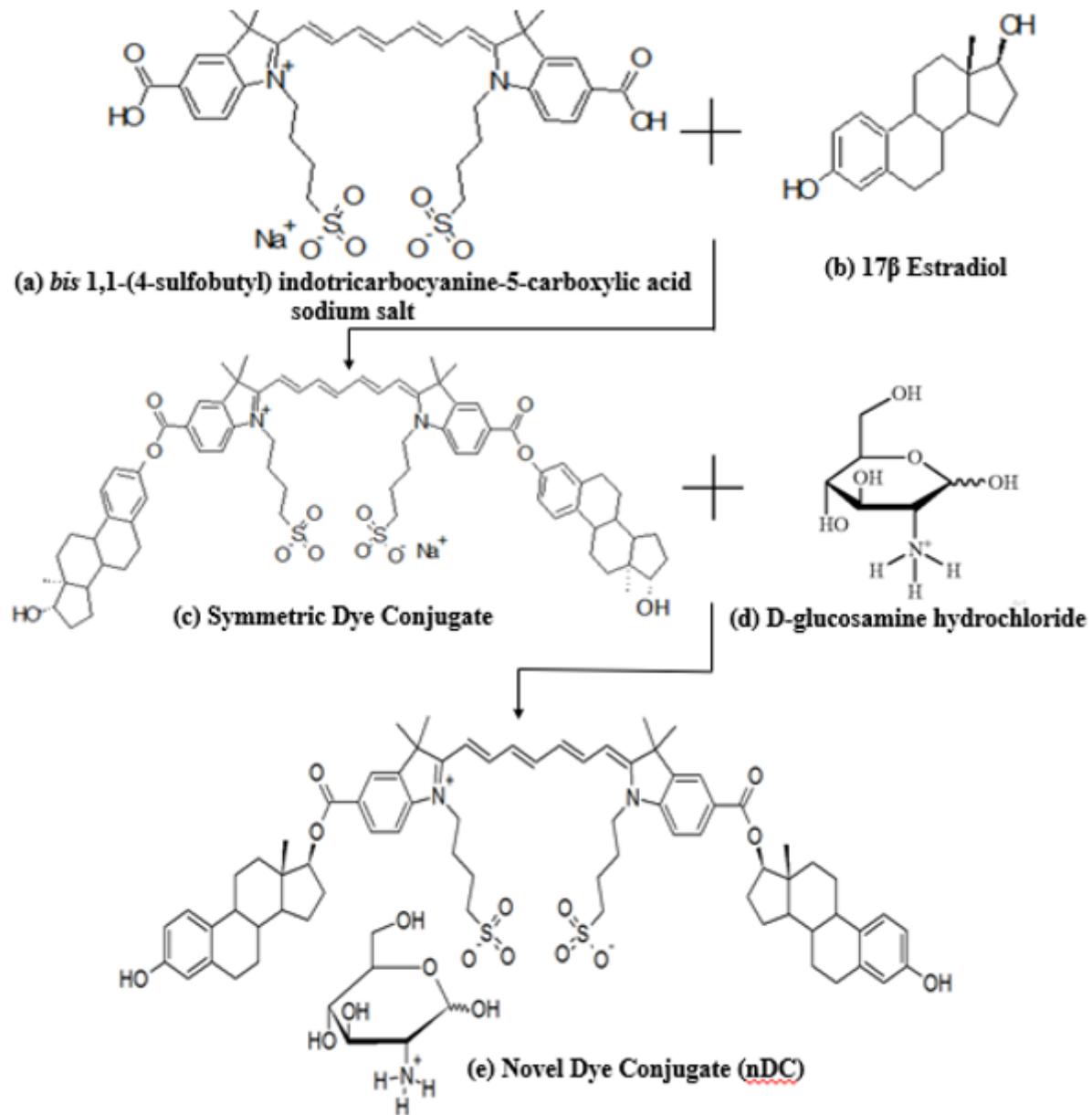
## Tables

TABLE 1

Photophysical Properties of nDC

Solvent	Absorption Maxima (nm)	Emission Maxima (nm)	Stokes's Shift
DMSO	757	787	30
PBS	755	788	33

## Figures



**Figure 1**

Synthesis steps: Conjugate of 17 $\beta$ -Estradiol with an analogue of ICG

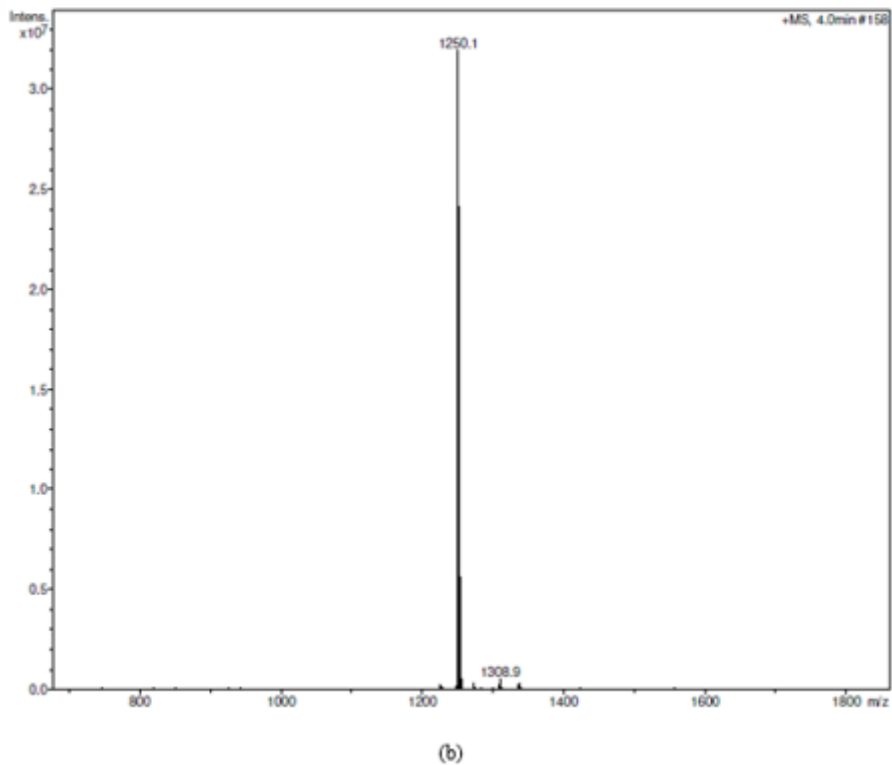
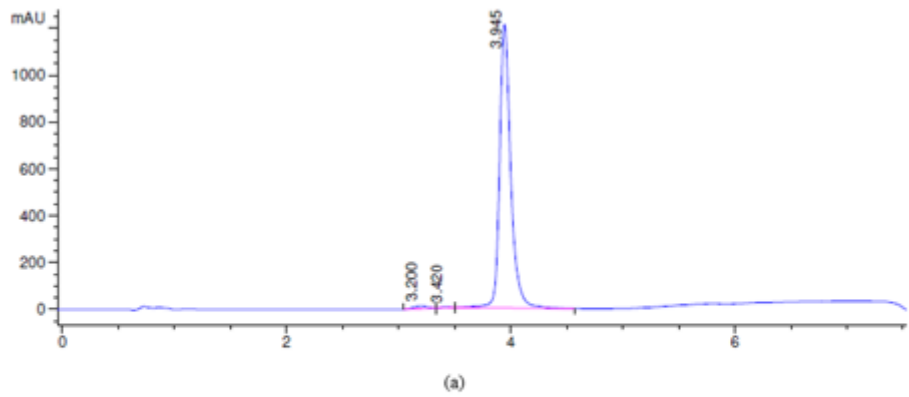


**Figure 2**

LC- MS report: (a) LC report and (b) Mass report

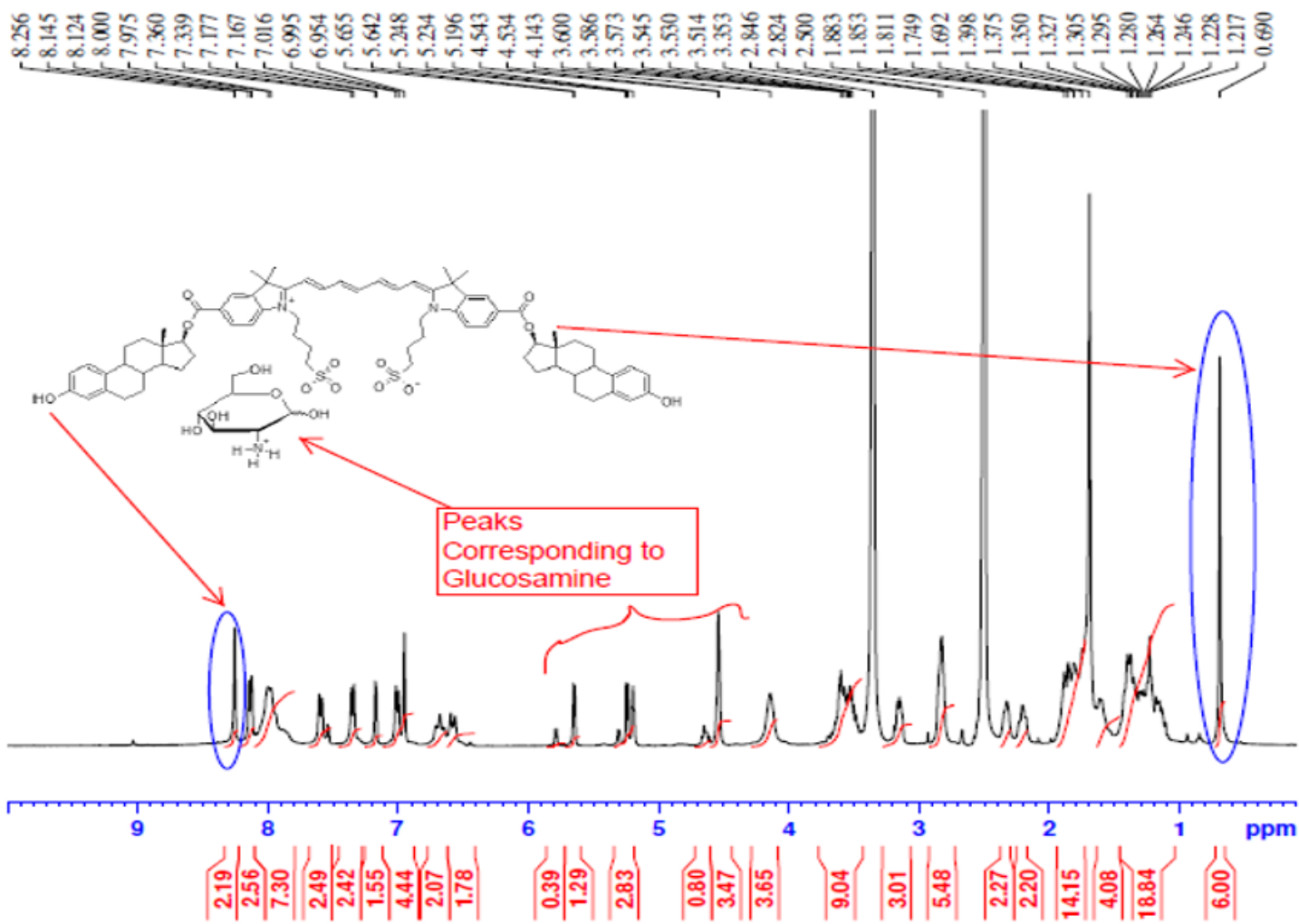


**Figure 3**

## **1H-NMR spectrum of nDC**

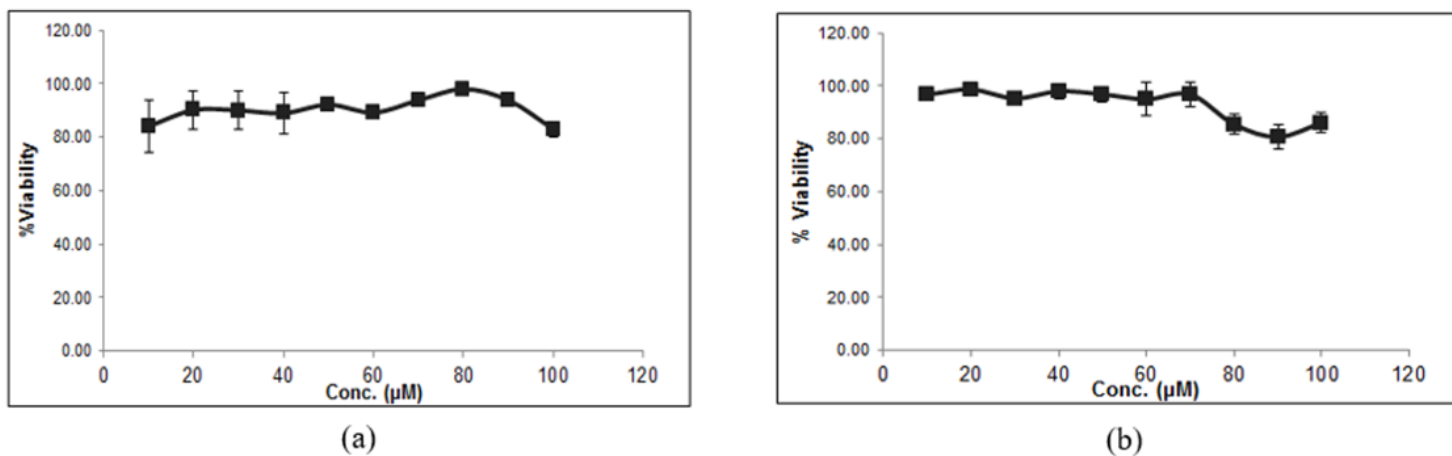


**Figure 4**

## nDC concentration vs Cell Viability in (a) MCF-7 and (b) MDA MB 231

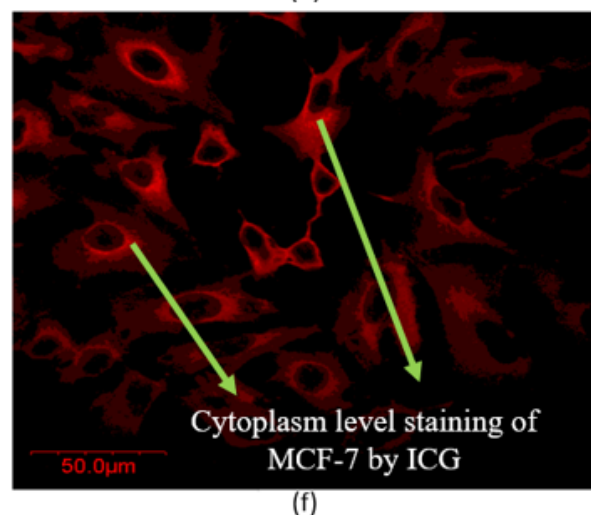
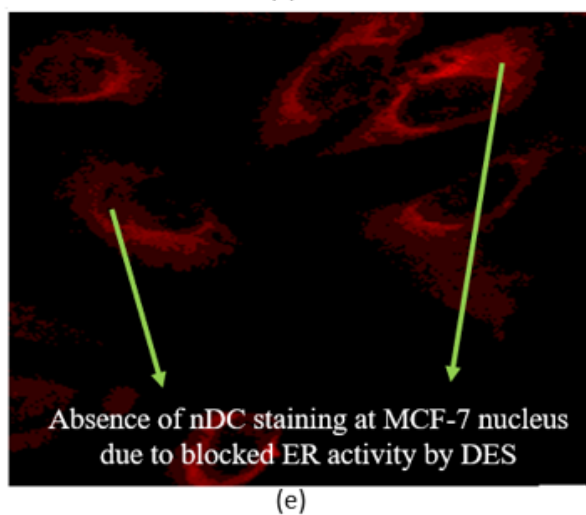
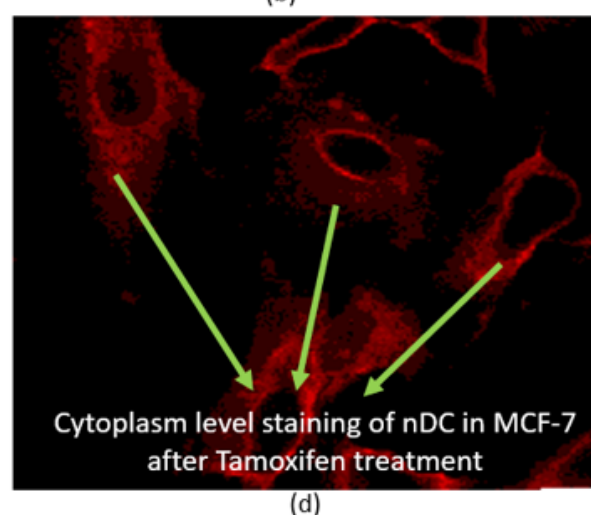
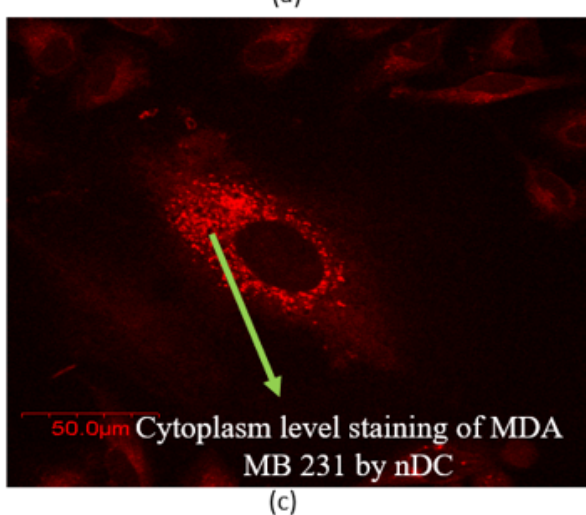
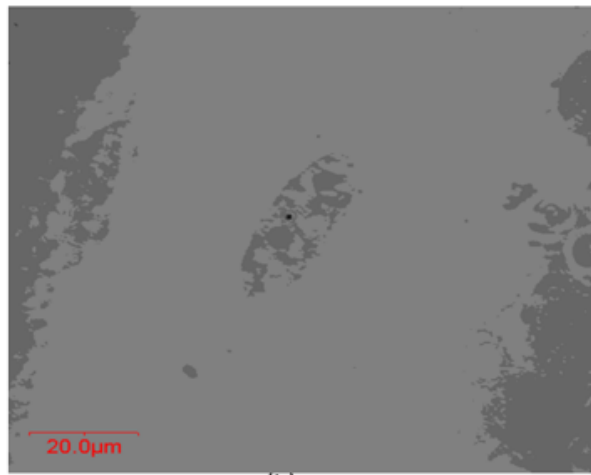
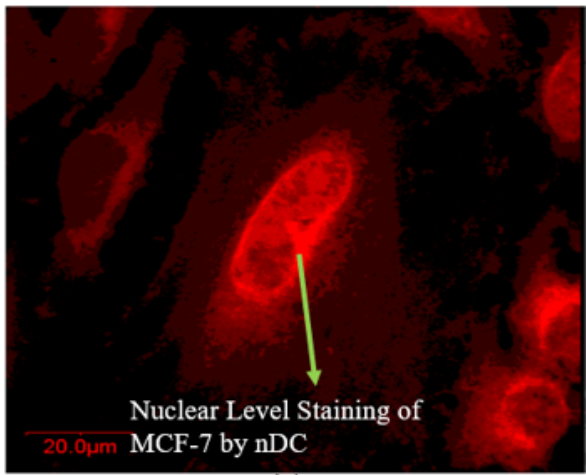


**Figure 5**

Confocal laser scanning microscopy images of cell line studies

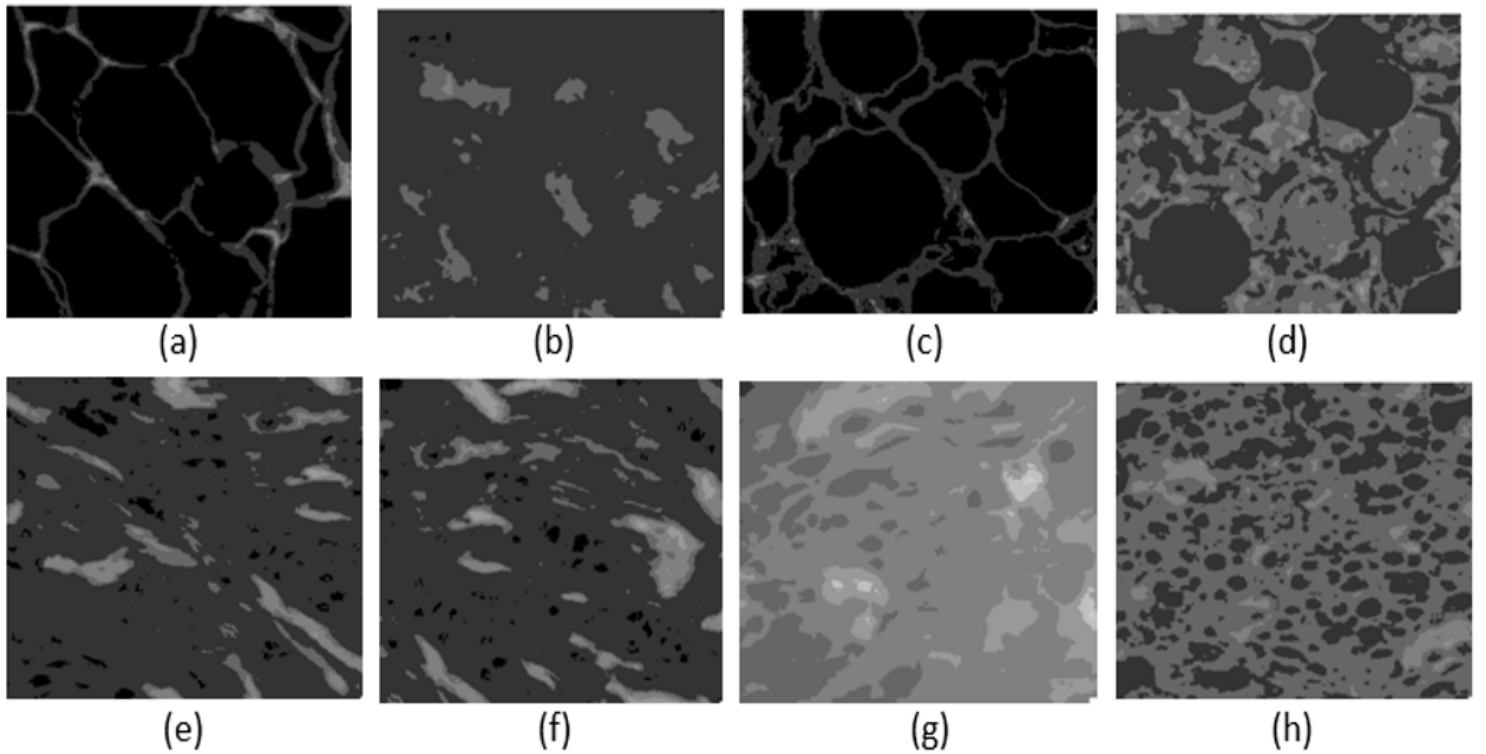


**Figure 6**

nDC ER binding of Non-Invasive Ductal Carcinoma: (a)The Control and (b)Specific binding nDC ER binding of Non-Invasive Lobular Carcinoma: (c)The Control, (d) Specific binding, (e,f) ER binding of Non-Invasive Adenocarcinoma, (g,h) ER binding of Non-Invasive Medullary Carcinoma